

# Rapid and Semi-automated Method for Analysis of the Number of Atoms of Ultra-small Platinum Clusters on Carbon

J.C. Yang,<sup>1\*</sup> S. Bradley,<sup>2</sup> and J.M. Gibson<sup>1</sup>

<sup>1</sup>Frederick Seitz Materials Research Laboratory, University of Illinois at Urbana-Champaign, Urbana, IL 61801

<sup>2</sup>UOP LLC, 50 East Algonquin Road, Des Plaines, IL 60017

**Abstract:** Very high angle (~100 mrad) annular dark-field (HAADF) images in a dedicated scanning transmission electron microscope (STEM) can be used to quantitatively measure the number of atoms in a cluster on a support material. We have developed a computer program which will automatically find the location of the particles and then integrate the intensity to find the number of atoms per cluster. We have examined ultra-small Pt clusters on a C substrate by this novel mass-spectroscopic technique. We discovered that the Pt clusters maintain their three-dimensional shape, and are probably spherical.

**Key words:** platinum, metal clusters, high angle annular dark-field, quantification, scanning transmission electron microscope, catalysis, nanoparticles

## INTRODUCTION

Catalysis is used in virtually all industrially important reactions—from oil-refining to manufacturing of clothing. Catalysis depends on surface chemistry. Therefore, it is vital to understand the structure of catalytic materials directly on their support material, since this will clearly affect their catalytic activity. Extended adsorption fine structure (EXAFS) is an excellent method in determining the bonding information for the catalytic material, but it provides only averaged information. For more detailed information, transmission electron microscopy (TEM) can provide in-

sights into the structure and chemistry, as well as their distribution of supported metal clusters (Prestridge et al., 1977). We have recently developed a mass spectroscopic technique using a scanning transmission electron microscope (STEM), which gives the number of atoms per cluster (Singhal et al., 1997). The concept of this technique is that the STEM images due to electrons scattered at extremely high angles are predominantly incoherent, regardless of the arrangement of the atoms. This method is typically referred to as high angle annular dark-field (HAADF) or Z-contrast imaging. Crewe et al. (1975) demonstrated the power of this technique to image single heavy atoms on a low-Z material. Nellist and Pennycook (1996) have demonstrated that high-resolution Z-contrast images provide information on the raft-like structure of the metal clusters on alumina. Treacy et al. (1980) demonstrated elegantly that the quantification of the relative intensity of the HAADF STEM images pro-

Received October 13, 1999; accepted January 3, 2000.

J.M. Gibson is now at Materials Science Division, Argonne National Laboratory, Argonne, IL 60439.

\*Corresponding author, at Department of Materials Science and Engineering, University of Pittsburgh, Pittsburgh, PA 15261.

vides unique information about the dimensionality of these ultra-small metal clusters. We extended this method to the measurement of the absolute scattered intensity and that provides the number of atoms in a cluster. The robustness of this technique was verified experimentally with Re-6 clusters dispersed on graphite, where the measured number of atoms was  $6 \pm 2$  Re atoms (Singhal et al., 1997). The combination of this novel mass-spectroscopic technique with other electron microscopy techniques can provide unique insights into the 3-D structure of these supported catalysts. As an example, we have previously studied a bi-metallic catalyst, PtRu<sub>5</sub> on carbon black, by a wide variety of electron microscopy techniques. We have demonstrated that the PtRu<sub>5</sub> clusters are raft-like on the carbon black support using this STEM-based technique (Yang et al., 1998). Here, we will present our results on analyzing ultra-small and dispersed Pt clusters on amorphous carbon.

## EXPERIMENT

The ultra-small Pt clusters on the amorphous carbon Cu grid were made by a proprietary technique. The Pt had poor interaction with the catalyst support and, during preparation using isopropanol, fell off of the catalyst support and decorated the grid.

Imaging for the STEM-based mass-spectroscopic technique was performed on a Field Emission Gun (FEG) VG HB601 STEM operated at 100 kV. The probe size used in our experiments was estimated at  $\sim 5\text{\AA}$ . Image analysis was performed on the unprocessed 16-bit digital images, where the absolute measured intensity from the clusters were converted to scattering cross-sections, which can then be converted to number of atoms:  $\sigma_{\text{tot}} = N\sigma_{\text{Pt}}$ .

### Z-contrast Method for Determining Number of Atoms

Image analysis was performed on the unprocessed 16-bit digital images. The integrated intensity for each particle is over a circular region sufficiently large to enclose the particle completely. In order to convert the results into absolute cross-sections ( $\text{\AA}^2$ ), we use the formula:

$$\sigma = \frac{T}{\mu_{\text{DF}}EN_0} \quad (1)$$

where  $T$  is the integrated signal ( $T = \sum_p I_p \delta_p$  where  $I_p$  is the intensity of pixel  $p$  and  $\delta_p$  is its area),  $\mu_{\text{DF}}$  is the annular dark field (ADF) detector efficiency,  $E$  is the image exposure time (sec), and  $N_0$  is the electron number flux density per second. The product  $\mu_{\text{DF}}N_0$  is the number of counts detected by the annular detector for an unscattered beam in 1 sec, and was measured as discussed below. Calibration of the scintillator-photomultiplier detector is a critical issue.

The beam current was measured by integrating over the zero-loss peak from parallel electron energy loss spectroscopy (PEELS). A manual stop was made such that the HAADF detector could be moved to a predetermined position. The beam current was lowered by a fixed amount (typically a factor of  $\sim 100$ ) compared to the incident beam current,  $I_{\text{high}}$ , used for acquiring the HAADF images in order to prevent saturation of the detector by the unscattered beam  $I_{\text{high}}$ , used during the image acquisition. After taking the images and lowering the electron current, the HAADF was moved to the predetermined position such that the electron beam would strike the HAADF. Line scans across the ADF images revealed a low detector efficiency near the inner edges and a higher efficiency at the less damaged outer regimes of the detector. Normalized detector counts/pixel ( $\mu_{\text{DF}}N_0^{\text{high}}$  for a known main beam current,  $I_{\text{high}}$ ), can be obtained by weighting the detector counts with the square of the atomic scattering factor,  $f(\theta)$  for a platinum atom from the inner (113 mrad) to the outer scattering angle (326 mrad) of the detector. Hence, the measured scattering cross-section is:

$$\sigma = \frac{T I_{\text{low}}}{\Delta^2 I_{\text{high}} N_{\text{mask}}} \quad (2)$$

Sigma is the scattering cross-section of the cluster which is the number of atoms times the scattering cross-section from one Pt atom. Delta is the pixel width.  $I_{\text{high}}$  is the current used during the measurements.  $I_{\text{low}}$  refer to the reduced current that is directly on the HAADF detector.  $N(\text{mask})$  is the normalized detector counts.

### Interactive C++ Program for Rapid Identification of Particles and Data Analysis

We have recently developed an interactive C++ program that will rapidly analyze HAADF images such as Figure 1. Figure 2 is the corresponding bright field (BF) image of the Pt clusters on C taken at 1 M. The diameters of the Pt

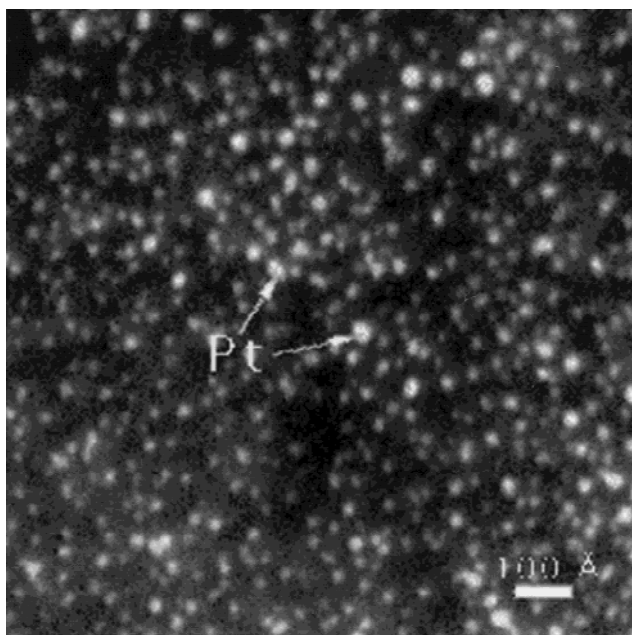


**Figure 1.** High angle annular dark field (HAADF) image of Pt clusters on C.

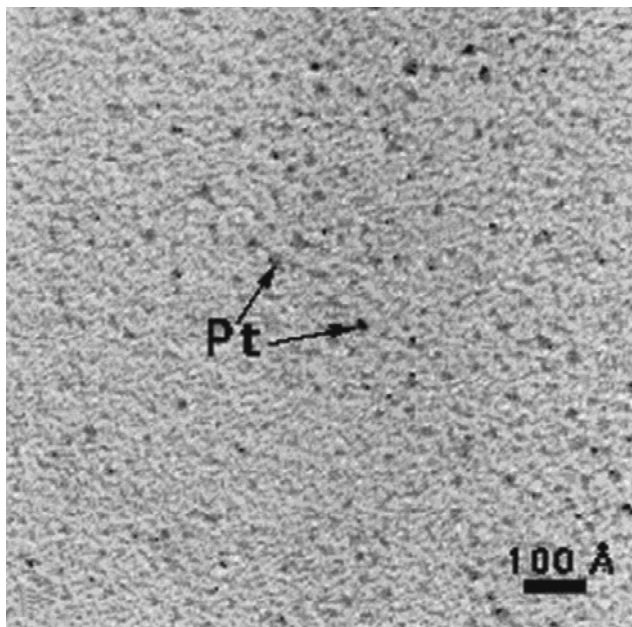


**Figure 2.** The corresponding bright field of Pt clusters on C.

clusters range from  $8\text{\AA}$  to  $25\text{\AA}$ . This method identifies the “good” particles for data analysis as “round,” by evaluating the eccentricity, and are not close to another particle. Once these particles have been identified, then the program analyzes these particles for their half-radius and integrated intensity. The half-radius is the radius where the integrated intensity is half the maximum integrated intensity. This

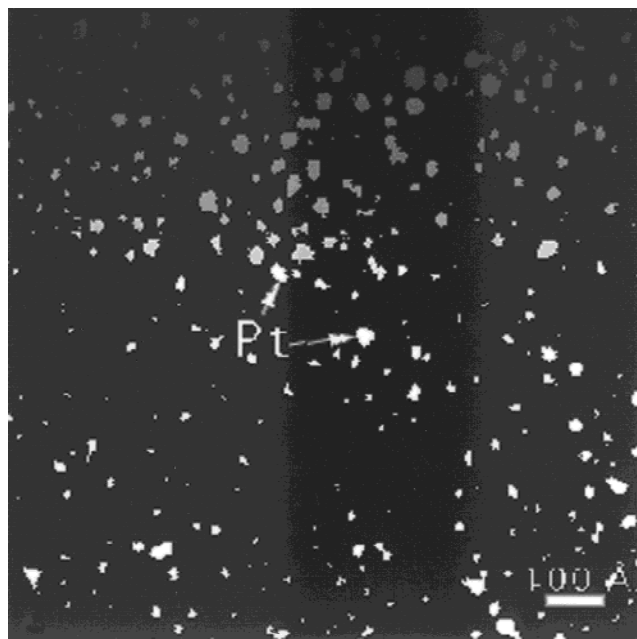


**Figure 3.** Thresholded image. The particles are numbered where the intensity of the particle in this image is its assigned number.

method was chosen as a more accurate method for experimentally measuring the particle size, as opposed to measuring the position of the maximum integrated intensity. Figure 3 is an example of the threshold image of Figure 2 where the “good” particles have been identified. Filtering of the image is also incorporated into the program in order to smooth the background for improved accuracy in the identification of particles.

Figure 4 shows an example of the integrated intensity vs. the integration radius for a spherical particle convoluted with a Gaussian probe, where the position of the half-radius is noted. The correlation between half-radius and the actual radius of the particle depends on the probe profile. If the probe size is considerably smaller than the particle size, then the measured radius is similar to the radius of the particle. If the probe size is about the same size as the particles (as is the case here), then the measured radius is significantly larger than the particle radius. Determination of the particle radius would require accurate knowledge of the probe profile during the time of the experiment.

## RESULTS

This interactive C++ program analyzed the integrated intensity and half-radius within several minutes on a Power Macintosh™ 7600. This sum was converted to number of atoms using equation (2) (Fig. 5).

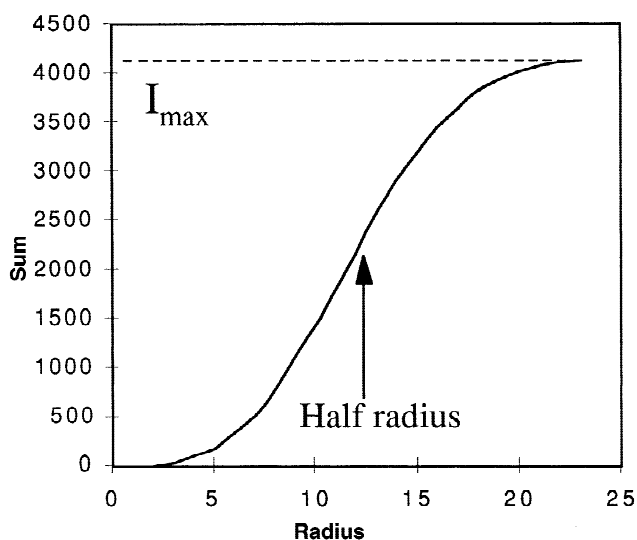


**Figure 4.** Integrated intensity (sum) vs. radius for a perfect sphere convoluted with a Gaussian probe. The position of the half-radius is indicated here.

The power dependence of the integrated intensity vs. the radius provides structural information. If the 2-D shape is maintained, then the power dependence would be 2, whereas for 3-D, the power law would be 3 (Fig. 4, solid line) (Treacy and Rice, 1989). However, the power law fit to this data is  $n = 4.06$ . To explain this unusually high power dependence, we examined the effects of the probe on our data. This effect of broadening the radius becomes greater when the particle size is close to the probe size. We simulated the integrated intensity for a sphere (with radius  $r$ ) with no probe convolution and a sphere with a Gaussian probe, where probe =  $(1/\pi\sigma^2)\exp(-r^2/2\sigma^2)$ ,  $\sigma = 3.6$  (Fig. 5, dotted line). We observe an excellent match with our experimental data when we consider probe effects on our intensity measurements. Hence, the Pt clusters maintain their 3-D shape. However, further work is needed to accurately determine the probe size and shape.

## DISCUSSION

By measuring the absolute intensity of very HAADF images and examining the effects of the probe shape, we demonstrated that ultra-small Pt clusters maintain their 3-D shape and are probably spherical. The probable reason why the Pt clusters maintain their 3-D shape is that they “fell off” the support material, indicating very little interaction with the support material, and most likely are spherical. It should be noted that the image of a sphere vs. a raft-like shape would

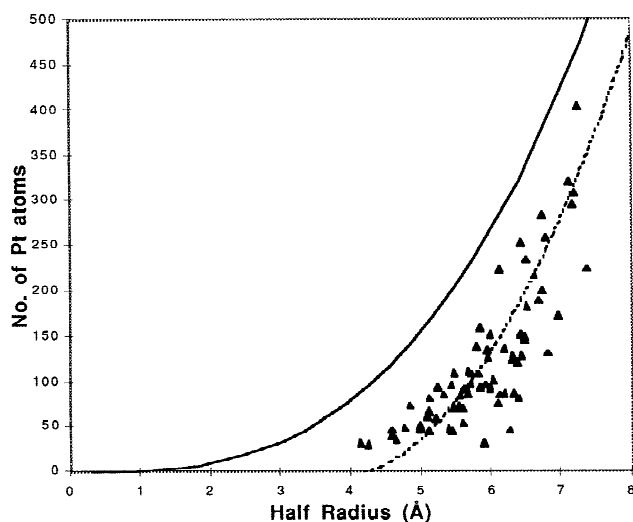


**Figure 5.** The integrated intensity vs. half-radius for nano-sized Pt clusters on C. The solid line corresponds to a sphere, and the dotted line corresponds to a Gaussian probe convoluted with a sphere.

appear qualitatively similar by plan-view TEM, but the quantification of the intensity provides deeper information about the supported structure.

Although the measurements of the integrated intensity is robust, measurement of the radius is difficult because of some uncertainty of the probe shape, which needs to be experimentally determined in order to accurately determine the shape, since the image is a convolution between the two. For example, using a probe with  $\sigma = 3.6\text{Å}$ , and spherical particle with radius  $10\text{Å}$ , then the measured half-radius of this particle will be  $7\text{Å}$ .

The specimens used for the experiments presented in this article were on a low-scattering support, i.e., carbon. However, this technique should also work with more realistic substrate materials, such as alumina, although the signal-to-noise ratio will worsen due to the increased scattering from the support material. One exciting potential is the determination of substrate effects on the structure of the supported cluster. Our initial results indicate that the Pt clusters interact more with the  $\gamma\text{-Al}_2\text{O}_3$  support than the C support. Another intriguing possibility is the discovery of magic numbers in ultra-small supported clusters, which have been theoretically predicted but not yet seen experimentally (Poltorak and Boronin, 1966).

## CONCLUSIONS

Using HAADF STEM images, we have demonstrated absolute mass measurement of stable ultra-small ( $8\text{Å}$ – $25\text{Å}$ ) Pt

clusters on amorphous carbon, and shown that the clusters maintain their 3-D shape and are probably spherical. We have also developed a robust interactive computer program to analyze this images rapidly. In-depth studies of the probe size and shape are important in determining the shape of the Pt clusters more accurately.

## ACKNOWLEDGMENTS

---

The authors thank Dr. Peter Miller for his invaluable help with the computer programs and Dr. Ajay Singhal (Applied Materials, Santa Clara, CA) for discussions about the Z-contrast technique. This project at the University of Illinois was supported by Department of Energy grant DEFG02-91ER45439, as well as the UOP, and involved extensive use of the facilities within the Center for Microanalysis of Materials of the Frederick Seitz Materials Research Laboratory.

## REFERENCES

---

- Crewe AV, Langmore JP, Isaacson MS (1975) Resolution and contrast in the scanning transmission electron microscope. In: *Physical Aspects of Electron Microscopy and Microbeam Analysis*. New York: Wiley, p 47
- Nellist PD, Pennycook SJ (1996) Direct imaging of the atomic configuration of ultradispersed catalysts. *Science* 274:413–415
- Poltorak OM, Boronin VS (1966) Mitohedry—a new method of studying active centres in crystalline catalysts. *Russ J Phys Chem* 40:1436–1445
- Prestridge EB, Via GH, Sinfelt JH (1977) Electron microscopy studies of metal clusters: Ru, Os, Ru-Cu and Ox-Cu. *J Catalysis* 50:115–123
- Singhal A, Yang JC, Gibson JM (1997) STEM-based mass spectroscopy of Re clusters. *Ultramicroscopy* 67:191–206
- Treacy MMJ, Howie A, Pennycook SJ (1980) Z contrast of supported catalyst particles in the STEM. EMAG 79, Institute of Phys. Conference Series
- Treacy MMJ, Rice SB (1989) Catalyst particle sizes from Rutherford scattered intensities. *J Microsc* 156:211–234
- Yang JC, Bradley S, Yeadon M, Gibson JM (1998) Nano-sized catalysts investigated by a STEM-based mass spectroscopic technique. *EMAG* 143:383–386